

Electrochemical Micromachining of Square Holes in Stainless Steel in H₂SO₄

Gu Mingcheng¹, Zeng Yongbin^{1,2,*}, Meng Lingchao¹

¹ College of Mechanical and Electrical Engineering, Nanjing University of Aeronautics and Astronautics, Nanjing 210016, China

² Jiangsu Key Laboratory of Precision and Micro-Manufacturing Technology, Nanjing 210016, China

*E-mail: binyz@nuaa.edu.cn

Received: 2 September 2018 / Accepted: 27 October 2018 / Published: 30 November 2018

A method for fabricating micro square holes with small corner radius is proposed, which could find applications in the aerospace and aviation industries. The machining process includes three steps: (i) the hole is first fabricated by electrochemical drilling; (ii) the square hole is then rough machined by electrochemical milling; and (iii) finally the hole is finished by electrochemical milling to reduce the corner radius. To improve the stability and quality of machining, double-pulsed electrochemical machining (ECM) was applied to remove electrolysis products adhering to the electrode. Using optimal parameters, square holes with a radius of 12 μm and a width of 100 μm were fabricated on 321 stainless steel with a thickness of 0.1 mm.

Keywords: electrochemical drilling; electrochemical milling; double-pulsed ECM; square hole; small radius

1. INTRODUCTION

With the development of microelectromechanical systems (MEMS), micromachining plays an ever-increasing and important role in the process of miniaturization of electrical and electronic equipment. In order to realize various special functions, many microstructures such as grooves, holes and slits have been widely used in MEMS. Micro holes, as prominent microstructures in micro devices, have been applied in various industrial applications. The progress made in the automobile [1], aviation and medical [2] fields has created an increasing need for the fabrication of micro holes in extremely hard and tough materials [3]. Because of their special mechanical properties, micro square holes have been adopted in the aerospace industry and in various instruments. However, the fabrication of micro square holes is a more difficult task than the machining of round holes because of the corner radius problem.

In order to meet the requirements for fabricating micro square holes in different applications, researchers have adopted various techniques to produce micro square holes [4], such as drilling [5], electrical discharge machining (EDM) [6], laser beam machining (LBM) [7], electrochemical machining (ECM) [8]. Dangra applied a cam containing a Reuleaux triangle, in which each vertex traces a curve that is almost a square when the cam rotates, to drill square holes [5]. The method is suitable for the machining of soft materials, but the size of the cam is limited. Therefore, micro square holes are more difficult to be fabricated by this method. EDM has been extensively adopted to satisfy the needs of mechanical fabrication, especially in micromachining, ever since wire electrical discharge grinding (WEDG) was proposed. Yu [6] proposed a micro-EDM called the uniform wear method, which realized the fabrication of square slots with sharp corners. Kim used LBM to machine square holes with optimal parameters in Si_3N_4 [7]. EDM and LBM are thermal processes, so there are always heat-affected zones and recast layers on the workpiece [8]. Damage to the workpiece should be avoided in many applications. The advantages of ECM make it eminently suitable for micro machining in aviation and aerospace applications [9]. Liu proposed micro electrochemical milling machining technology to fabricate complex structures [10]. Liu applied electrochemical drilling with electrode jump motion to machine holes on stainless steel with a thickness of 0.5 mm [8]. Hewidy researched the effect of the low frequency vibration of a pipe electrode on the fabrication of holes in electrochemical machining [11]. It is difficult for ECM to ensure the precision of holes because of the machining gap. Considering the various disadvantages of the different techniques described above, a new method for fabricating micro square holes with small corner radii is herein proposed.

Our investigations were focused on the fabrication of micro square holes on 321 stainless steel by ECM. In order to increase the efficiency and reduce the corner radius, the method involved both rough milling and finish milling. The purpose of finish milling is to modify square holes in order to reduce the corner radius. The stability and quality of machining was improved by adopting double-pulsed ECM. The effects of different machining parameters such as applied voltage, pulse duration and pulse period were investigated. Using optimal parameters, square holes with corner radii of 12 μm and a width of 100 μm were fabricated on 321 stainless steel with a thickness of 0.1 mm.

2. EXPERIMENTAL

The cardinal technical target of square hole is the corner radius. To achieve a square hole with a radius below 15 μm , a new method of fabrication is proposed. The process of fabricating micro square holes includes three steps: (i) the fabrication of micro holes by electrochemical micro drilling with tool jump motion; (ii) the rough machining of square holes by electrochemical milling; and (iii) the finish milling of the square holes. To reduce the clamping error, the method applied multiple, stepped, cylindrical micro electrodes to produce the square hole without replacement of the electrode and workpiece in the machining process. In order to maintain the stability of machining, double-pulses were adopted to eliminate products formed on the electrode.

Fig. 1 shows the experimental setup, which consisted of a power supply, a servo-controlled feed unit, a PZT (piezoelectric ceramics) unit, an oscilloscope and a charge-coupled device (CCD) [12]. In

order to improve precision and reduce the size of the hole, ultra-short voltage pluses were applied throughout the entire machining process. In our experiments, we used a cylindrical tungsten electrode as the cathode and a 321 stainless steel with a thickness of 0.1 mm as the anodic workpiece. The electrolyte was 0.1 M aqueous H₂SO₄.

2.1 Electrochemical drilling

The difficulty with micro electrochemical drilling is how to remove dissolution products and renew the electrolyte in the machining gap. In order to improve the transport of electrolysis products, electrochemical drilling with tool electrode jump motion is proposed. The principle of electrochemical drilling is illustrated in Fig. 1. The electrolyte in the machining gap can be refreshed by the high accelerating motion of the tool electrode and the low frequency vibration of the workpiece. Fig. 2 shows the motion of the electrode in the machining cycle, in which the jump motion of the electrode is used to renew the electrolyte, and the electrochemical reaction occurs during the slow feeding of the electrode. The workpiece vibrates along the axial direction of the cylindrical electrode and the highest point of motion is the stationary position of the workpiece, which is beneficial to disrupt the flow field and to remove electrolytic products [12]. The displacement of the workpiece is clearly described in Fig. 3.

2.2 Electrochemical milling

The same experimental system was used in electrochemical drilling and milling processes. The principle of electrochemical milling is illustrated in Fig. 1. The square hole with a width of 100 μm and a corner radius below 15 μm could not be directly fabricated, so a method was proposed that took two steps to mill the square hole.

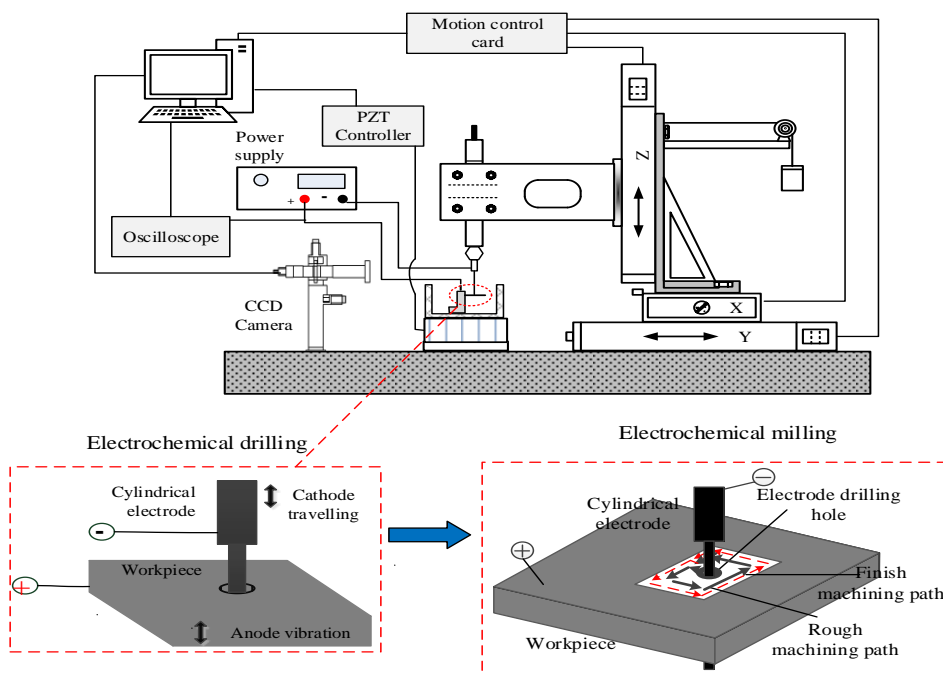


Figure 1. Schematic diagram of experimental system

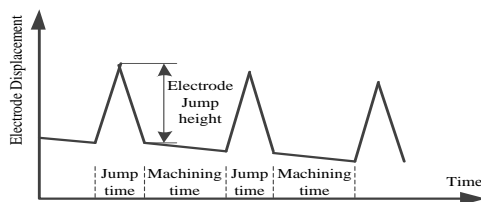


Figure 2. Diagram of the electrode displacement

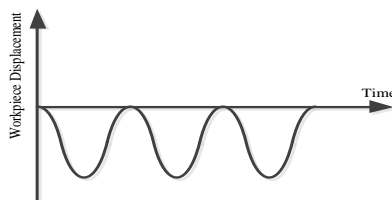


Figure 3. Diagram of the workpiece displacement

First, the cylindrical electrode is moved down about $60\ \mu\text{m}$ to avoid a taper after electrochemical drilling, and large machining parameters are adopted to mill the square hole in the specified trajectory. Second, small-optimized parameters are applied to modify the square hole to the required precision.

3. RESULTS AND DISCUSSION

In our study, the fabrication of micro square holes includes electrochemical drilling, rough milling and finish milling. The hole fabricated by electrochemical drilling was convenient for the following machining. Rough machining was used to remove material effectively, and finish machining was adopted to reduce the corner radius. The effects of the machining parameters on the square hole were then investigated.

3.1 Investigation of electrochemical drilling

The hole was machined by electrochemical drilling with multiple, stepped, cylindrical micro electrode. Fig. 4 illustrates the principle of the cylindrical electrode's in situ fabrication. The tungsten rod linked to the anode of the power supply was immersed in 2 M KOH solution and the stainless steel plate was the cathode in electrochemical etching. When the machining voltage was applied, electrochemical reactions occurred at the tungsten rod [10]. The diameter of the forepart of the cylindrical electrode was about $10\ \mu\text{m}$.

Electrode jump motion is useful for refreshing the electrolyte and removing products from the machining gap. Pre-trials were carried out as described in Reference [8]. Finally, the optimal machining conditions were found to be: feed rate of $0.1\ \mu\text{m s}^{-1}$, applied voltage of 10 V, pulse duration of 100 ns, pulse period of $1\ \mu\text{s}$, electrode jump height of 5 mm, electrode jump speed of $4\ \text{mm s}^{-1}$ and electrolyte concentration of 0.1 M H_2SO_4 . The hole fabricated with optimized parameters on 321 stainless steel is shown in Fig. 5. The diameter of hole was $52\ \mu\text{m}$.

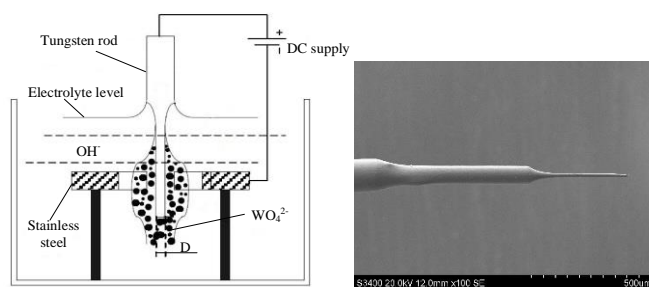
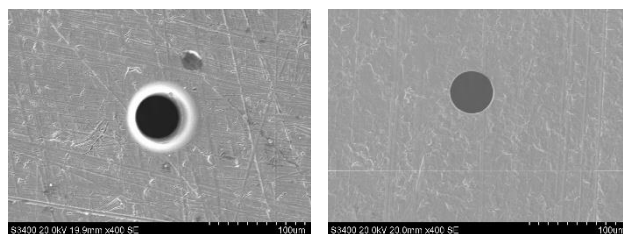


Figure 4. Sketch of the cylindrical electrode fabricated in situ



(a) Upper surface

(b) Lower surface

Figure 5. Scanning electron microscopy (SEM) images of the hole fabricated by electrochemical drilling (applied voltage = 10 V, feed rate of $0.1 \mu\text{ms}^{-1}$, pulse duration = 100 ns, pulse period = 1 μs , electrode jump height = 5 mm, electrode jump speed = 4 mm s^{-1} and H_2SO_4 electrolyte concentration = 0.1 M. (a) Upper surface (b) Lower surface)

3.2 Investigation of rough milling

In rough milling, high efficiency is the main aim, but stability is also important. On the premise of ensuring the stability of machining, the feed rate should be as large as possible. Therefore, double-pulsed ECM was adopted to dissolve the products on the electrode in order to improve the stability of machining. The effects of feed rate and double pulses were investigated.

3.2.1 Effect of double pulses

The key to maintaining the stability of machining is to remove electrolysis products from the machining gap as they are formed. Zeng presented three approaches to enhancing mass transport, that is, electrolyte flushing along the wire, the ring wire travelling in one direction and micro-vibration of the cathode wire [13]. Due to the size and shape of the electrode, the above methods could not be used in our experiments. The electrolysis products easily accumulate on the electrode without enhancement of mass transport, which leads to frequent electric short circuits. Thus, double-pulsed ECM was adopted to eliminate products adhering to the electrode. The difference between single and double-pulsed ECM is depicted in Fig. 6. The workpiece acts as the anode, and the cathode is the electrode in single-pulsed ECM. However, the electrode acts as the cathode during the pulse-on time and as the anode in the pulse-off time (known as the reverse-pulse time) in double-pulsed ECM.

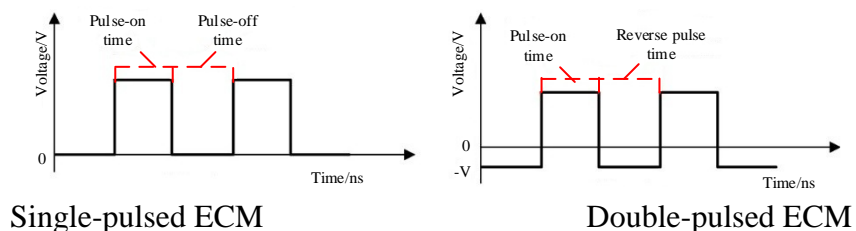


Figure 6. Difference between single-pulsed ECM (left) and double-pulsed ECM (right)

The machining conditions were: pulse-on voltage of 10 V, pulse period of 1.0 μs , pulse-on time of 100 ns, feed rate of 0.4 $\mu\text{m s}^{-1}$ and H_2SO_4 electrolyte concentration of 0.1 M. The value of the negative voltage played a key role in double-pulsed ECM. When the magnitude of the negative voltage was too small, the electrolysis products on the surface of electrode could not be completely removed, which meant that there was no obvious improvement in machining quality. Moreover, the large negative voltage led to dissolution of the electrode. The slits fabricated at different negative voltages are shown in Fig. 7. It can be seen that the machining quality was poor when the negative voltage was below -0.3 V due to the products remaining on the electrode. Therefore, the appropriate negative voltage for machining was chosen to be -0.3 V .

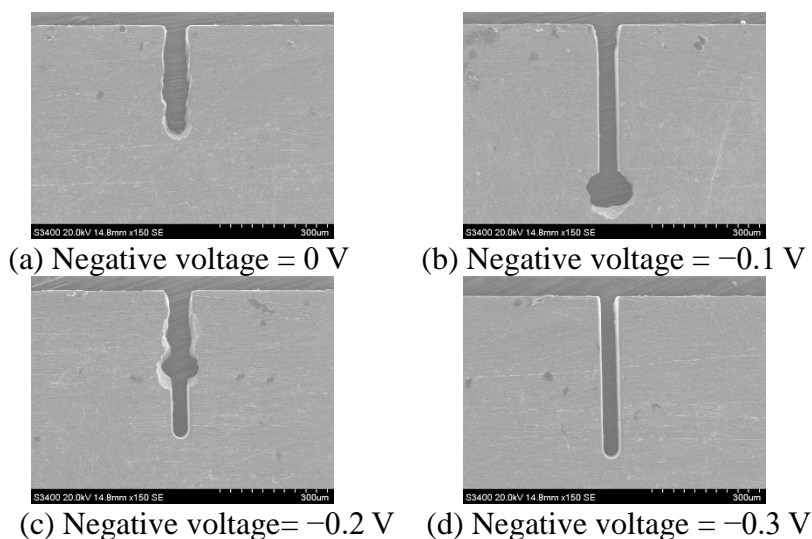


Figure 7. Scanning electron microscopy (SEM) images of slits at different negative voltages (pulse-on voltage = 10 V, pulse period = 1.0 μs , pulse-on time = 100 ns, feed rate = 0.4 $\mu\text{m s}^{-1}$ and H_2SO_4 electrolyte concentration = 0.1 M. (a) Negative voltage = 0 V. (b) Negative voltage = -0.1 V . (c) Negative voltage = -0.2 V . (d) Negative voltage = -0.3 V .)

3.2.2 Effect of feed rate

The constant machining parameters were: applied voltage of 10 V, -0.3 V , pulse-on time of 100 ns, pulse period of 1 μs and 0.1 M H_2SO_4 . Fig. 8 shows that the side gap increased as the feed rate

decreased from 0.4 to 0.1 $\mu\text{m s}^{-1}$. Frequent electric short circuits occurred when the feed rate was greater than 0.4 $\mu\text{m s}^{-1}$. According to ECM theory, an increase in feed rate results in a reduction in the machining balance gap, all other parameters being constant, while the machining balance gap is proportional to the side gap [14]. As the side gap was too small, it was not capable of maintaining machining stability because it was difficult to remove products from the machining area. Thus, there is a maximum value of the feed rate in machining when other parameters are constant. In order to achieve high efficiency and a stable process, the optimal feed rate was determined to be 0.4 $\mu\text{m s}^{-1}$.

The optimized parameters in rough machining, which are: applied voltage of 10 V with -0.3 V, pulse period of 1 μs , pulse-on time of 100 ns, feed rate of 0.4 $\mu\text{m s}^{-1}$ and H_2SO_4 electrolyte concentration of 0.1 M, can be acquired by experiments. The corner fabricated with optimized parameters is shown in Fig. 9. The width of the slit was 58 μm and the corner radius was 30 μm .

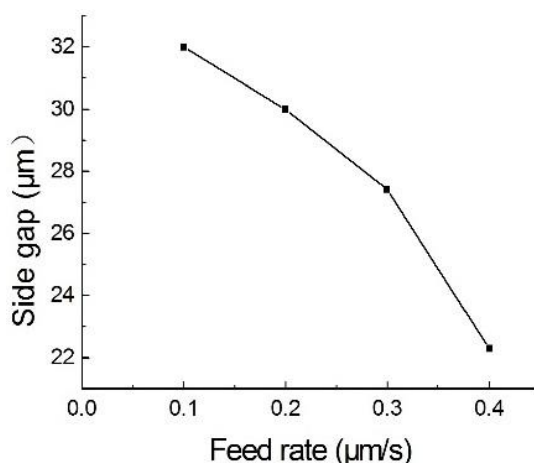


Figure 8. Variation in width of side gap with feed rate (applied voltage =10 V with -0.3 V, pulse period = 1 μs , pulse-on time = 100 ns, feed rate = 0.4 $\mu\text{m s}^{-1}$ and H_2SO_4 electrolyte concentration =0.1 M)

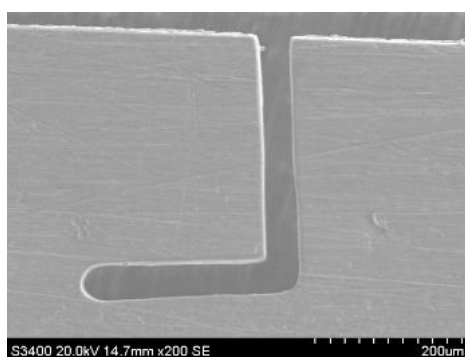


Figure 9. Corner fabricated by rough machining

3.3 Investigation of finish milling

The corner radius is an important technical target for square hole fabrication and should be as small as possible. However, the radius fabricated by rough milling with optimal parameters was greater

than 15 μm . To reduce the corner radius, finish milling was applied to modify the square hole. The process of machining is depicted in Fig. 10, where ‘ d_0 ’ is defined as the distance between electrodes and straight edges of the slit fabricated by rough milling, ‘A’ and ‘B’ are the tangent point of the corner machined in rough milling. The effects of machining parameters on the radius were also investigated.

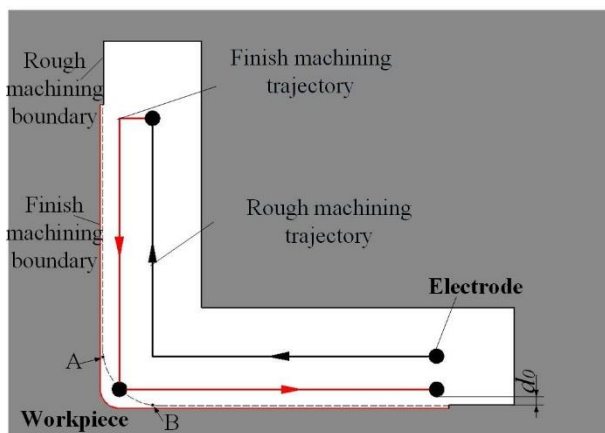
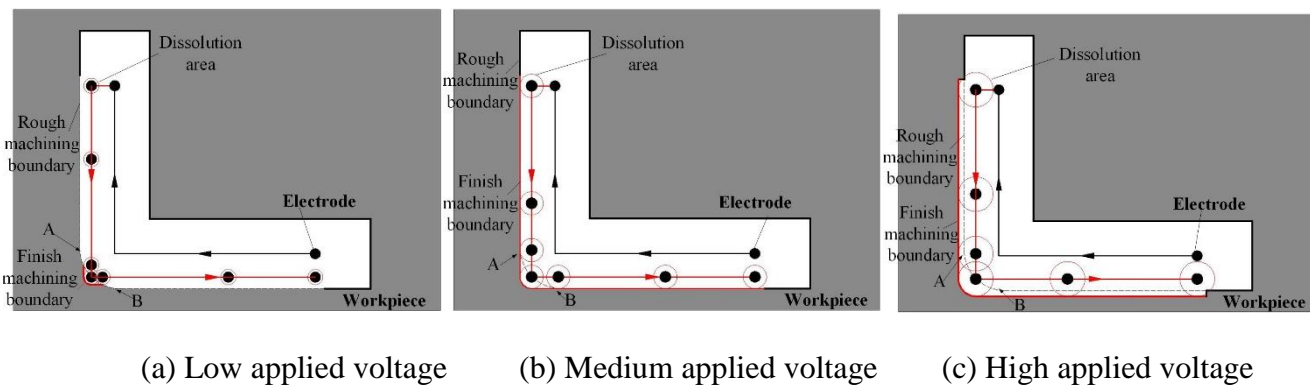


Figure 10. Schematic diagram of the finish milling

3.3.1 Effect of applied voltage on the corner radius



(a) Low applied voltage (b) Medium applied voltage (c) High applied voltage

Figure 11. The schematic diagram of corner modified in different applied voltages

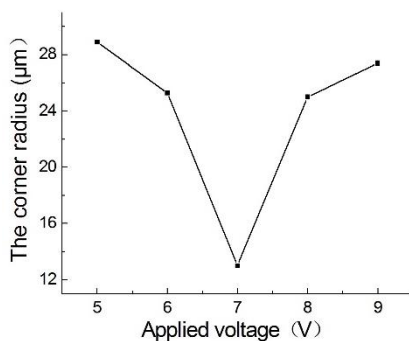


Figure 12. Variation in the corner radius with applied voltage (pulse duration = 100 ns, pulse period = 1.6 μs , feed rate = 0.4 $\mu\text{m s}^{-1}$, $d_0=5 \mu\text{m}$ and H_2SO_4 electrolyte concentration = 0.1 M)

The fixed machining parameters were: pulse duration of 100 ns, pulse period of 1.6 μs , feed rate of 0.4 $\mu\text{m s}^{-1}$, $d_0=5 \mu\text{m}$ and H_2SO_4 electrolyte concentration of 0.1 M. The schematic diagrams of corner modified in different applied voltage are shown in Fig. 11. It can be seen from Fig. 11(a) that when applied voltage is low, the electrochemical reaction doesn't always occur during \widehat{AB} . The corner consists of several circle arc and it is irregular. According to the double layer theory of pulsed ECM, the current density between electrode and workpiece increases with an increase in applied voltage, resulting in the increase of dissolution rate [14]. The dissolution area expands with the increase of applied voltage, leading to the increase of removal material during \widehat{AB} and the reduction of corner radius. This is why the corner radius decreases as applied voltage increases from 5 to 7V in Fig. 12. When the dissolution area is tangent to the boundary of slit, there is material removal in whole \widehat{AB} and the corner radius is decided by the radius of dissolution area, just like the one shown in Fig. 11(b). If applied voltage increases further, the straight edge of slit would be dissolved. Meanwhile, the corner radius is equal to the radius of dissolution area. It can be seen from Fig. 12 that the radius increases with the increase of applied voltage from 7 to 9V. In order to achieve a small corner, an applied voltage of 7 V was determined to be optimized.

3.3.2 Effect of pulse duration on the corner radius

These experiments were carried out with constant parameters: applied voltage of 7 V, pulse period of 1.6 μs , $d_0=5 \mu\text{m}$, H_2SO_4 electrolyte concentration of 0.1 M and feed rate of 0.4 $\mu\text{m s}^{-1}$. It can be seen from Fig. 13 that the corner radius first decreases and then increases as the pulse duration increases from 80 to 120 ns. The increase of pulse duration means the increase of charging time of double layer, leading to the expansion of dissolution area. When the pulse duration is 80 ns, electrochemical reaction only occurs in the part of \widehat{AB} and the reduction of corner radius is not obvious. As pulse duration increases from 80 to 100 ns, the removed material in \widehat{AB} increases and the corner radius reduces. If the dissolution area is big enough to contain point A and B, the corner radius is the radius of dissolution area. Thus, the corner radius increase as pulse increases from 100 to 120 ns. The optimal value of the pulse duration was determined to be 100 ns.

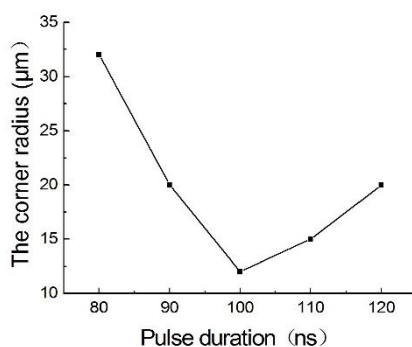


Figure 13. Variation in the corner radius with pulse duration (applied voltage = 7 V, pulse period = 1.6 μs , feed rate = 0.4 $\mu\text{m s}^{-1}$, $d_0=5 \mu\text{m}$ and H_2SO_4 electrolyte concentration = 0.1 M)

3.3.3 Effect of pulse period on the corner radius

The machining parameters were as follows: applied voltage of 7 V, pulse duration of 100 ns, H₂SO₄ electrolyte concentration of 0.1 M, $d_0=5\ \mu\text{m}$ and feed rate of $0.4\ \mu\text{m s}^{-1}$. From Fig. 14, it can be seen that the smallest radius can be acquired in 1.6 μs . The pulse duration was fixed at 100 ns, that is, the time for charging was the same in different pulse periods. However, the average reaction current per unit time changed with the variation in pulse period. The longer the pulse period is, the smaller the average reaction current is. The dissolution area is decided by the average reaction current, namely, the dissolution area expands as pulse period decrease. As pulse period is below 1.6 μs , the dissolution area would contain point A and B. The corner radius totally depends on the radius of dissolution area. However, if the pulse period was over 1.6 μs , the radius of corner increases with the increase of pulse period because of the decrease of dissolution rate. Thus, a pulse period of 1.6 μs was determined to be optimal.

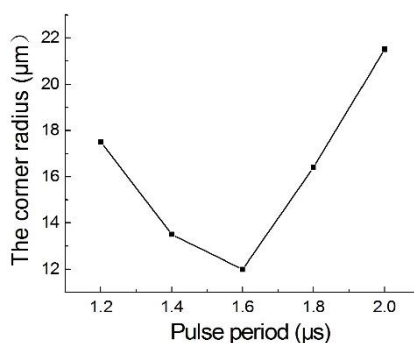


Figure 14. Variation in the radius of the corner with pulse period (applied voltage = 7 V, pulse duration= 100 ns, feed rate = $0.4\ \mu\text{m s}^{-1}$, $d_0=5\ \mu\text{m}$ and H₂SO₄ electrolyte concentration = 0.1 M)

3.3.4 Effect of feed rate on the corner radius

The effect of feed rate on the corner radius was studied with the following fixed machining parameters: applied voltage of 7 V, pulse duration of 100 ns, pulse period of 1.6 μs , $d_0=5\ \mu\text{m}$ and H₂SO₄ electrolyte concentration of 0.1 M. The change in the corner radius with increasing feed rate can be seen from Fig. 15. According to Faraday's law, the reaction time per unit distance decreased with an increase in the feed rate, resulting in a decrease in the amount removed per unit distance. In other words, the dissolution area shrinks as feed rate increase. If the amount removed per unit distance was large, point A was contained in the dissolution area and the corner was totally modified in finish machining. The radius of corner is up to the radius of dissolution area, so the corner radius decrease as the feed rate increase from 0.2 to $0.4\ \mu\text{m s}^{-1}$. When the feed rate increased from 0.4 to $0.6\ \mu\text{m s}^{-1}$, the corner radius increased because of the reduction of removal amount per unit distance. The optimal feed rate was determined to be $0.4\ \mu\text{m s}^{-1}$.

The optimized parameters of finish machining were as follows: applied voltage of 7 V, pulse duration of 100 ns, pulse period of 1.6 μs , $d_0=5\ \mu\text{m}$, H₂SO₄ electrolyte concentration of 0.1 M and feed rate of $0.4\ \mu\text{m s}^{-1}$. The modified corner is shown in Fig. 16.

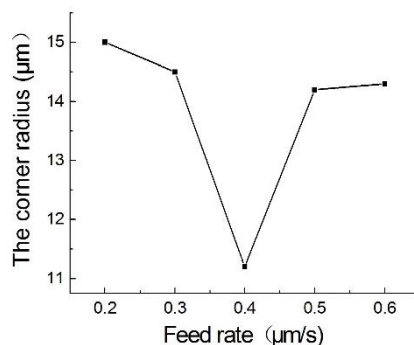


Figure 15. Variation in the radius of the corner with feed rate (applied voltage = 7 V, pulse duration= 100 ns, pulse period = 1.6 μs, $d_0=5 \mu\text{m}$ and H_2SO_4 electrolyte concentration = 0.1 M)

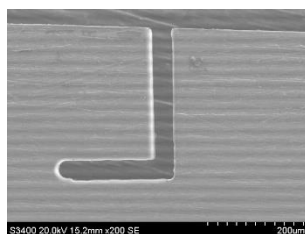
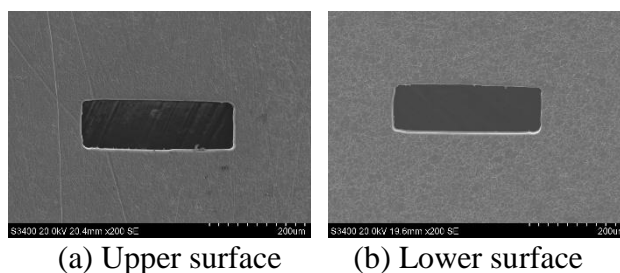


Figure 16. The modified corner

3.4 Fabrication of the square hole

The fabrication of the square hole consists of three steps: (i) fabrication of the micro hole by electrochemical micro drilling with tool jump motion; (ii) machining of the abrasive square hole by electrochemical milling; and (iii) finish machining of the square hole. Following the investigation of the effects of different parameters on the machining of the square hole, the latter was fabricated using the optimized parameters. The machining conditions of the first step were: feed rate of $0.1 \mu\text{m s}^{-1}$, applied voltage of 10 V, pulse duration of 100 ns, pulse period of 1 μs, electrode jump height of 5 mm, electrode jump speed of 4mm s^{-1} and H_2SO_4 electrolyte concentration of 0.1M. The parameters of the second step were as follows: applied voltage of 10 V with -0.3V , pulse duration of 100 ns, pulse period of 1 μs, feed rate of $0.4 \mu\text{m s}^{-1}$ and H_2SO_4 electrolyte concentration of 0.1 M. The machining conditions of finish machining were: applied voltage of 7 V, pulse period of 1.6 μs, pulse duration of 100 ns, H_2SO_4 electrolyte concentration of 0.1 M, feed rate of $0.4 \mu\text{m s}^{-1}$ and $d_0=5 \mu\text{m}$. The square hole fabricated with optimized parameters is shown in Fig. 17. The radius of the hole decreased from 30 to 12 μm.



(a) Upper surface (b) Lower surface

Figure 17. Square hole fabricated by ECM

4. CONCLUSIONS

This paper has investigated the fabrication of square holes on 321 stainless steel by ECM. The fabrication process comprises three steps: (i) a micro hole is first fabricated by electrochemical drilling with electrode jump motion; (ii) the rough square hole is machined by electrochemical milling; and (iii) the square hole is modified by milling to reduce the corner radius. Experiments were carried out to study the influence of some key parameters on the formation of the square hole. The conclusions drawn from these experiments can be summarized as follows:

1. Double-pulsed ECM can reduce the amount of products adhering to the electrode and improve the stability and quality of machining. There is an appropriate negative voltage in machining.
2. Finish machining can raise the level of precision and reduce the corner radius. The combination of rough and finish machining is suitable for fabricating micro square holes.
3. A square hole with a width 100 μm and a corner radius of 12 μm was successfully fabricated in 321 stainless steel of thickness 0.1 mm.

ACKNOWLEDGEMENTS

This project was supported by the National Natural Science Foundation of China (51775276), and the Special Research Project of Civil Aircraft(MJ-2016-G-71).

References

1. L. Li, C. Diver, J. Atkinson, R. Giedl-Wagner and H.-J. Helml, *CIRP Annals - Manufacturing Technology*, 55 (2006) 179.
2. D. Landolt, P.F. Chauvy and O. Zinger, *Electrochimica Acta*, 48 (2003) 3185.
3. D. Zhu, Y.B. Zeng, Z.Y. Xu and X.Y. Zhang, *CIRP Annals - Manufacturing Technology*, 60 (2011) 247.
4. T. Masuzawa, *CIRP Annals - Manufacturing Technology*, 49 (2000) 473.
5. S. Dangra and S. Dangra, *International Journal of Engineering Development and Research*, 5 (2017) 1621.
6. Z. Yu, T. Masuzawa and M. Fujino, *Korea–Russia International Symposium on Science & Technology*, 3 (2000) 102.
7. K. Kim, J. Park, M. Bae and C. Lim, High efficiency laser square hole drilling of Si₃N₄ substrates, *Proceedings of Academics World International Conference, Edinburgh, UK, 2017*, 2320
8. Z. Liu, Z.J. Qiu, C. Heng and N.S. Qu, *Materials Science Forum*, 626 (2009) 333.
9. X. Wang, X. Fang, Y. Zeng and N. Qu, *International Journal of Electrochemical Science*, 11 (2016) 7216.
10. Y. Liu, D. Zhu and L. Zhu, *International Journal of Advanced Manufacturing Technology*, 60 (2012) 977.
11. M.S. Hewidy, S.J. Ebeid, T.A. El-Taweel and A.H. Youssef, *Journal of Materials Processing Technology*, 189 (2007) 466.
12. K. Xu, Y.B. Zeng, P. Li, D. Zhu, *Journal of Materials Processing*, 222 (2015) 103

13. Y.B. Zeng, Q. Yu, S.H. Wang and D. Zhu, *CIRP Annals - Manufacturing Technology*, 61 (2012) 195.
14. H.D. He, Y.B. Zeng and N.S. Qu, *Precision Engineering*, 45 (2016) 285.

© 2019 The Authors. Published by ESG (www.electrochemsci.org). This article is an open access article distributed under the terms and conditions of the Creative Commons Attribution license (<http://creativecommons.org/licenses/by/4.0/>).